MODELING THE IMPACT OF CONTAINER MATERIAL AND GEOMETRY ON THE UNIFORMITY OF DOSE IN IRRADIATION CALIBRATION

by
Marcus Snedeker

July, 2024

Director of Thesis: Dr. Regina DeWitt

Department: Department of Physics

ABSTRACT

In order to calibrate radiation sources in instruments used by the Optically Stimulated Luminescence Laboratory at ECU, samples are sent in containers to an external gamma source to be irradiated with a known radiation dose. The type of material used for the container can have an effect on the uniformity of dose absorbed by the sample, which can introduce unforeseen sources of error in the calibration. In this study, simulations were performed using DosiVox (via Geant4) to approximate the dose absorbed throughout different sample-container setups. The goal is to quantify dose uniformity and determine which container materials may be used, while still maintaining feasible levels of uniformity. It was ascertained that the container materials which best maintain uniformity for ceramic samples are aluminum, silica, and ceramic. It was also ascertained that the container materials which best maintain uniformity for silica samples are borosilicate glass, silica, and ceramic. Teflon was found to be the container material that maintained uniformity the least for both sample types.

Modeling the Impact of Container Material and Geometry on the Uniformity of Dose in Irradiation Calibration

A Thesis
Presented to the Faculty of the Department of Physics

EAST CAROLINA UNIVERSITY

In Partial Fulfillment of the Requirements for the degree
MS in Physics with a concentration in Applied Physics

By
Marcus SNEDEKER
July, 2024

Director of Thesis: Dr. Regina DEWITT, PhD in Physics

Thesis Committee Members:
Dr. Mark SPRAGUE, PhD in Physics
Dr. Michael DINGFELDER, PhD in Physics
Dr. Guglielmo FUCCI, PhD in Mathematical Physics

Dedicated to the friends who carried me through: *Charlie Suarez Reyes, Tehya Armstead, Alyssa Horne, Mason Ross, Joe Figueroa, Victor Aguilar, John Ascencio, and Marc Andalecio.*

Without them, I would not have made it through my time in North Carolina.

Acknowledgements

Throughout the duration of this project, I have had loads of help and support from many people. As such, I would like to thank the physics faculty at ECU and my thesis committee.

Namely Dr. Michael Dingfelder, who gave me a chance in 2021, and Dr. Regina DeWitt, for believing in my ability to complete this work and for her extreme patience in seeing it through.

Table of Contents

Acknowledgements iv

List of Tables vi

List of Figures vii

1 Motivation 1
- 1.1 Motivation for Thesis . . . 1
- 1.2 Thesis Overview . . . 3

2 Theory 4
- 2.1 Interaction of Gamma Radiation with Matter . . . 4
- 2.2 Optically stimulated luminescence . . . 7

3 DosiVox 10
- 3.1 Description of the DosiVox software . . . 10
- 3.2 Input file . . . 11
  - 3.2.1 Example Input File (ptf) . . . 14
- 3.3 Output File . . . 18
  - 3.3.1 Example Result File . . . 19

4 Parameterization and basic simulations 20
- 4.1 Optimizing matrix dimensions . . . 21
- 4.2 Edge Effects and horizontal cross sections . . . 26
  - 4.2.1 Analysis . . . 29

5 Data Analysis 31
- 5.1 Apparatus for Data Analysis . . . 31

6 Results 35
- 6.1 The Uniformity of Different Setups . . . 35
- 6.2 Conclusion . . . 37
  - 6.2.1 Future Directions . . . 38

Bibliography 40

List of Tables

4.1 R^2 Values by Dimension 23

6.1 Ceramic Sample Results 36
6.2 Silica Sample Results 36

List of Figures

2.1 Photoelectric Effect 5
2.2 Compton Scattering 6
2.3 Pair Production 7
2.4 Band Energy Diagram 8

3.1 Example of DosiVox Model 13
3.2 Example of a Result File 19

4.1 Photo of a Container 20
4.2 Matrices (15x15, 35x35, and 45x45) 22
4.3 Regression Coefficients 24
4.4 Times Chart 25
4.5 Statistical Relevance 25
4.6 Cross Section 26
4.7 Silica - Ceramic 27
4.8 Ceramic - Silica 28
4.9 Ceramic - Ceramic 29

5.1 Cross Section 32

Chapter 1

Motivation

1.1 Motivation for Thesis

In certain research labs at ECU, samples are irradiated by instruments containing radiation sources. These sources need to be calibrated in order to maintain accurate measuring ability of the instruments.

One set of such instruments are utilized in the study of optically stimulated luminescence (OSL), which is a method of measuring the radiation dose absorbed by minerals. Such a method may be used for the purposes of dating or dosimetry.

In OSL, incoming wavelengths of incident light stimulate mineral samples, and the samples then emit light of a different wavelength in the form of luminescence. The intensity of this resultant luminescence is proportional to absorbed dose. To properly elucidate this correlation between luminescence intensity and dose, samples must be irradiated with a known dose from a laboratory source of known dose rate.

Although radioactive sources (most commonly ^{90}Sr beta sources) come with information from the manufacturer on the activity and radionuclide, the source's actual dose rate depends on the geometry of the irradiation setup and the physical characteristics of the sample. As a

result, calibration of these sources is required. To perform this calibration, samples are sent to an external radiation facility (e.g. NIST) to be irradiated with a known dose of gamma radiation from ^{60}Co or ^{137}Cs. The samples are brought back to the lab where luminescence is measured. These measurements are then used to determine the amount of irradiation time by the uncalibrated source that is needed to produce the same luminescence signal as the known gamma dose. The resulting time is used to calculate a calibrated dose rate for the source in question.

Sample materials are loose grains or thin cylindrical slices of solid mineral samples or rocks. These samples need to be filled in a container. During measurement, OSL is obtained from an entire rock slice or alternatively ~ 100 grains that could have been located anywhere in the container. Thus, it is imperative that samples are irradiated with as much uniformity as possible to avoid variation of dose between different grains/slices, as variation would skew the average dose measured. One such factor that can affect dose uniformity is the difference between the sample and its container. During exposure to gamma radiation electrons are freed throughout container and sample. However, the number of electrons depends on atomic composition and density of a material. At the transition from one material into another there will likely be edge effects. These effects are particularly strong at the transition from thin air into a dense material, and the container has therefore the function to establish secondary electron equilibrium. However, there is another transition from container into the actual sample. In addition, the container wall will also absorb part of the radiation and decrease the dose. A detailed discussion can be found in [1].

To circumvent this problem, the samples have been placed in containers of the same (or similar) material. However, this can be difficult to do for samples made of certain rocks or granular samples. Thus, it would be advantageous to find a commercially available material that would have an overall minimal effect on the irradiation of certain sample types. The goal of this project is to investigate the extent to which differing container materials and

sizes influence the uniformity of dose absorbed during gamma irradiation, and to quantify dose and dose heterogeneity. To achieve this, Monte Carlo simulations were performed for various sample-container setups.

1.2 Thesis Overview

This work will start with a chapter (Chapter 2) discussing the theory behind gamma interactions with matter, and how that might apply to the irradiation of samples used in OSL studies.

Next in Chapter 3, the tool used for modeling and simulating the irradiation of samples (DosiVox) will be described in detail. Included are an example of the input file used to specify what is being simulated, and an example of an output file with the resultant data.

DosiVox defines the simulation geometry through a 3D matrix of rectangular subvolumes (voxels). This introduced issues in the setup of the cylindrical sample containers. The tests conducted to parameterize and optimize the simulations used in this study will be discussed in Chapter 4. This includes testing the efficacy of using more or less particles, and testing what resolution of voxels is optimal.

DosiVox provides dose values along a vertical cross-section in the setup. Multiple probe positions have to be simulated for a more detailed picture of the dose distribution in the container, and the individual results have to be combined. The analytical apparatus for determining dose uniformity within a sample and its level of variance will be discussed in Chapter 5.

Lastly, the results of different sample-container combinations will be discussed and analyzed in Chapter 6, as well as the direction future studies may take.

Chapter 2

Theory

The main purpose behind this project is to evaluate, which container materials and sizes provide the best dose uniformity in the sample when irradiated with a gamma source. As explained above, the irradiated samples are used to calibrate built-in sources for OSL dosimetry. This chapter explains how gamma photons interact with matter and gives a brief overview of the OSL phenomenon in general.

2.1 Interaction of Gamma Radiation with Matter

Crystal lattices are repeating arrangements of atoms held together via electromagnetic forces [2]. These atoms are mostly empty space with a nucleus in the center and electrons orbiting around the center. The radius of the first electron orbital is on the order of 10^4 times larger than the radius of any atom's nucleus. As such, any incoming photons are more likely to interact with an electron in its orbital than with the nucleus itself. Binding energies of electrons to the nucleus are on the order of eV, while photon energies are on the order of keV.

Photons interact with the electrons in three different ways:

Photoelectric effect

When a photon interacts with one of these outer electrons in such a way that it imparts energy onto it, the electron can either be raised to a higher (less stable) orbital or be freed from the atom entirely. This phenomenon is referred to as the *photoelectric effect* [3].

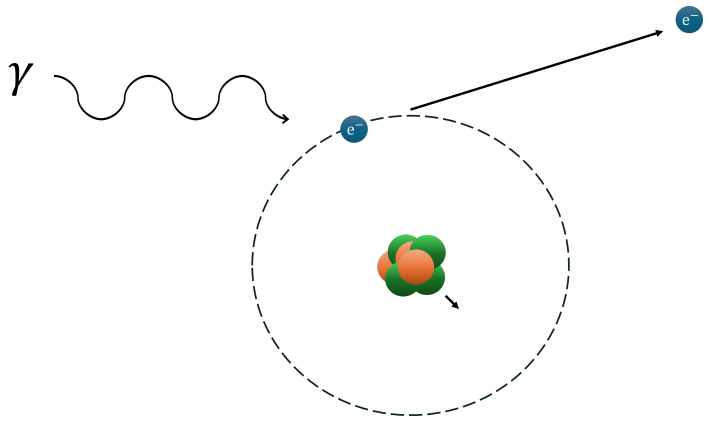

FIGURE 2.1: An illustrated example of the photoelectric effect.

Compton Scattering

Another form of gamma interaction is Compton scattering. When a gamma photon interacts with an electron and is not absorbed, it imparts a portion of its energy onto the electron while still maintaining enough to "scatter" off in another direction as a photon with a longer wavelength [4].

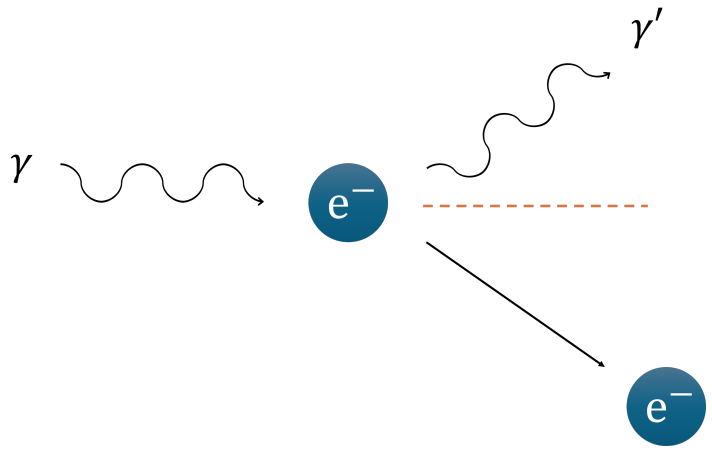

FIGURE 2.2: An illustrated example of Compton Scattering. Here, time is flowing from left to right, the incoming photon is represented by γ, and the scattered photon by γ'.

Pair Production

When a gamma photon enters an electric field, there is a nonzero probability of it spontaneously converting into two leptons of opposite charge (an electron and a positron) in a process called *pair production*. This can be the result of a nucleus' electric field, where the minimum energy required for the interaction is $E \geq 2m_e c^2$. This process may be represented by the following equation.

$$\gamma \rightarrow e^- + e^+$$

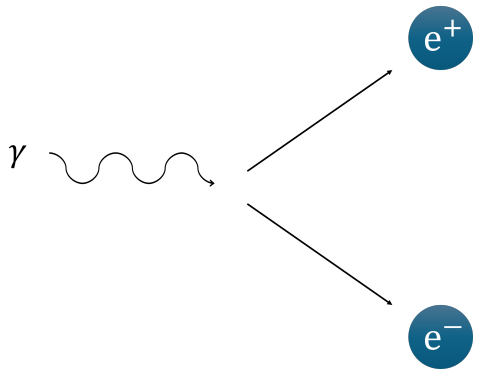

FIGURE 2.3: An illustrated example of pair production. Here, time is flowing from left to right. An incoming photon (represented by γ) spontaneously produces a positron-electron pair.

The energy imparted on these electrons is what contributes to the dose absorbed.In all three cases the free electrons have usually enough energy to release secondary and tertiary electrons through Coulomb interaction. The freed electrons can roam about the crystal and can become trapped in crystal deformities (traps). This is the basis for optically stimulated luminescence.

2.2 Optically stimulated luminescence

The main purpose behind this project is to calibrate instruments for the use of luminescence dosimetry. This particular phenomenon consists of electrons absorbing and emitting light under certain conditions.

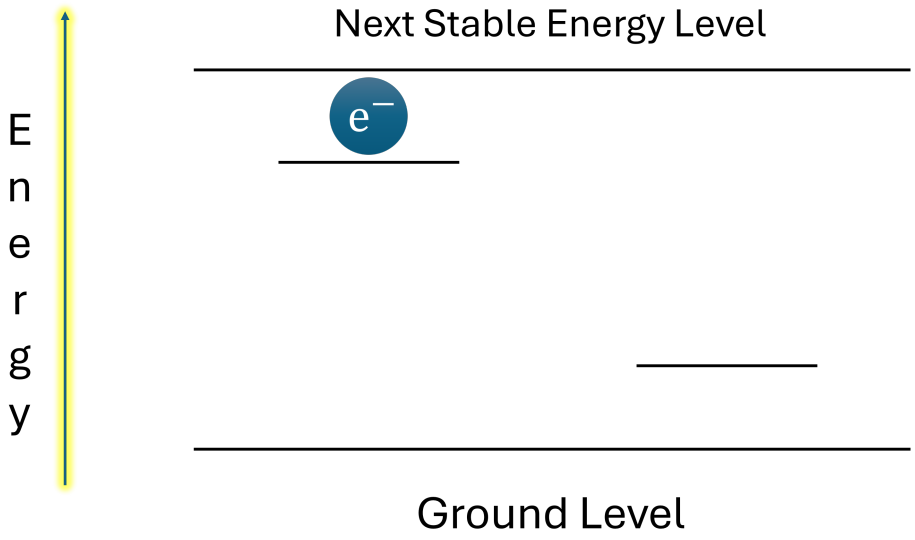

FIGURE 2.4: An energy band diagram wherein an electron is shown to be trapped in a higher-energy, unstable crystal defect.

Within a real crystal lattice, there tend to be defects. When the crystal is exposed to ionizing radiation, electrons absorb energy and are lifted from the ground level to the next higher energy band. There, the electrons are free to migrate through the crystal lattice until they either recombine with an ion or until they are trapped in a crystal defect, as seen in the energy band diagram shown in Figure 2.4 above [5]. The number of trapped electrons is directly correlated with the absorbed dose.

To provide enough energy for such electrons to be released, the crystal must be illuminated with incident light. The electron is released from its trap and can recombine with an ion. In this process a photon is emitted, and the emitted light is called *luminescence*. These luminescent photons are measured in the form of light intensity. This intensity can then be considered proportional to the number of trapped charges released, and is thus proportional to absorbed dose [1].

Different materials have a different number of defects intrinsic to their crystalline structures, and thus will have different luminescent intensities. As such, a correlation between dose and intensity must be established for each different material, which requires irradiation with a well-calibrated source of known dose. Radiation sources built into commercial luminescence readers need to be calibrated against a reference gamma source. To this end, samples are sent to a reference facility such as NIST. To minimize calibration errors, there must exist a high level of uniformity throughout a sample upon irradiation. The goal of this study is to quantify this uniformity and test the dose uniformity of various sample geometries and setups commonly used, and infer which setup will least affect the precision of the calibration of a source used in OSL measurement.

Chapter 3

DosiVox

In order to investigate the irradiation of sample-container setups of different materials and sizes, and to properly quantify dose uniformity, Monte Carlo simulation were performed via a Unix based program called DosiVox [6]. The following gives a more in depth look at the code used, the input files, and the output files.

3.1 Description of the DosiVox software

DosiVox is a Geant4 based program [6] that models the irradiation of user specified samples in various geometries and performs dose-rate calculations. No prior programming experience with Geant4 is required. Instead, Geant4 libraries are used [6], which are a set of open-source C++ codes compiled to model the interaction of particles passing through matter, and which are provided by CERN [7]. To specify samples, users write up a pilot text file (ptf) that will be fed into the DosiVox software to produce simulations. An example of such a ptf is included in Section 3.2.1.

In order to simulate the irradiation of samples in DosiVox, the user specifies the geometry of the sample in units of voxels, which are cubic volumes of user-specified material composition.

The geometry is determined by layers of matrices of these voxels. The material can be a solid cube to represent a solid sample, or it can be a cubic volume of randomly placed spheres of randomized radius in order to represent grains for sedimentary samples. Here, each voxel was considered to be solid, but 3 different materials were used to simulate container, sample and the surrounding air.

Physical properties of these materials (chemical composition, radioactivity, density and percentage of water content) may be specified.

DosiVox also has different types of detectors that can be simulated. In this study, the cylindrical detector was used. This detector runs the length of the simulated environment from top to bottom, and takes measurements based on a number of user-specified breaks. It will thus determine the dose along a vertical line at specific positions in the sample setup (usually in all the voxels along its length) [8]. In order to determine the vertical profile at another position a new ptf file has to be created and the simulation has to be run again.

3.2 Input file

An example pilot text file is shown below. This specific example was used in some of the earlier parametrization tests.

Users can specify how many radioactive particles are simulated and the source of radiation (e.g. Uranium, Potassium, Thorium) [lines 3 - 5]. Every particle is followed through all interactions until its remaining energy is so small that its projected range is below a certain cutoff value (here 0.001 mm [Line 5]). At that point all the remaining energy is simply deposited in the respective voxel. The simulation only records the energy that is deposited in a detector voxel. Other voxels are only included for calculating the path of a particle, but

their absorbed energy is not recorded. In this study, the cylindrical detector was used. [Lines 6 and 7].

There are 18 (with index numbers starting from 0) preset materials that DosiVox has in its library, such as ceramic and silica [Lines 8 and 9]. If a user wants to simulate a compound not included in that set of preset materials, they may create them by indicating the atomic composition and density of the compound and giving it an index. This index must start from 18, since the 17 and below represent the preset compounds [Line 11].

In the next section, the physical properties of these materials (such as density and percentage of water content) may be specified. The user first gives the material an index starting from 0 [Line 13], names the material [Line 14], and specifies the density and water content [Lines 15 and 16].

The number of components must be given [Line 17], then the component index and its percentage of dry mass [Line 18]. Last in this section, granulometry may be indicated in the form of the grain's physical properties [Lines 20 and 21]. This section is repeated for each material used in the simulation [seen in Lines 24 - 43].

The number of of voxels can be listed in the order of x, y, z [Line 45], and their sizes in $[mm]$ in the same order [Line 46].

The next portion of this document is the composition of the medium. To conduct simulations in DosiVox, users approximate objects in their immediate surroundings by separating them into layers where each voxel is assigned an index material. These assignments form a matrix indicating the location and material of each voxel in that layer. The layers are then spread from top to bottom according to the location of that layer in the height of the model. DosiVox simulates an environment based on these matrices, an example of which is shown below in Figure 3.1.

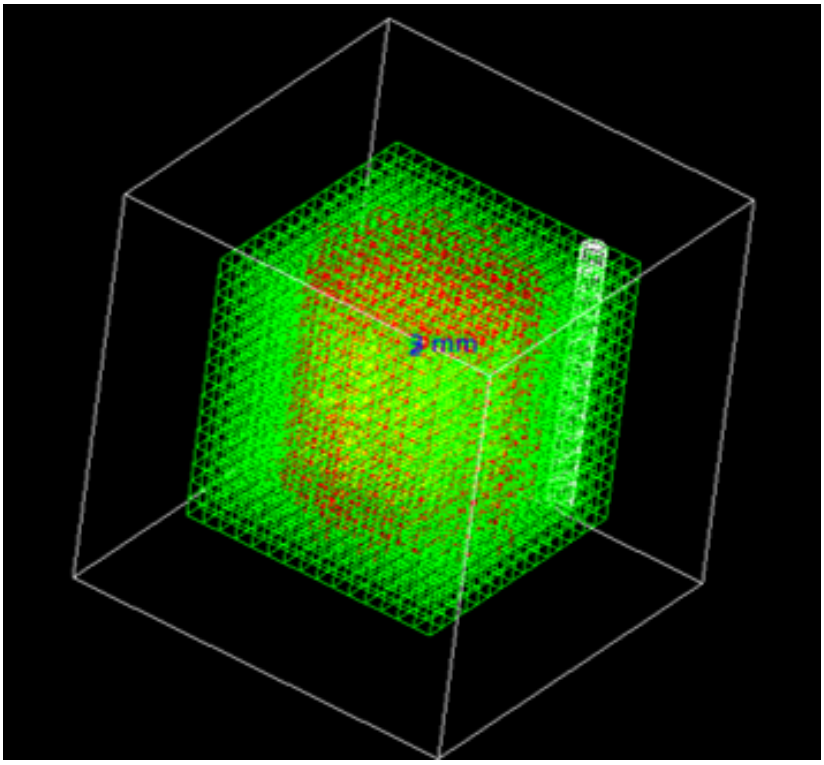

FIGURE 3.1: Visualization of the voxelization of sample and container. The surrounding air is represented by green voxels, the container by red voxels, and the sample by yellow voxels. The white long cylinder indicates the probe that measures a vertical profile of the dose.

The next section repeats the same matrices, but instead of material indices, users specify which voxels are radiocactive. The number 0 stands for a non-radioactive voxel. Integer numbers stand for radioactive voxels, where the activity scales with number (e.g. 2 has twice as much activity as 1), [Lines 51 - 66].

Lastly, the user specifies the detector size and location within the voxel(s) which it occupies [Lines 70 and 71].

3.2.1 Example Input File (ptf)

```
1. FileName #result file name
2.
3. 10000.  1 # ( x 1000 ) emitted particles, clock value (%)
4. 3 0 0 0 #particle emitted:  1 for alpha, 2 for beta, 3 for
   gamma ; momentum of emission in X,Y,Z directions (0 0 0 for
   random direction)

5. 0 0.001 #element emitter (1 for uranium series, 2 for tho-
   rium series, 3 for potassium, 0 for User Defined), cut in
   range value (mm)
6. 0 13 -1 1 #index for detector definition, detector voxel,
   material for mapping, emission from grains
7. 5 1 50.  50.  #number of probe cells, probe diam (mm), probe
   offset in X and Y (in % of voxel X,Y sizes)
8. 0 #number of new components defined
9. 3 #number of materials used
10.
11. 18 _B2O3 2.46 2 B 2 O 3
12.
13. 0 # material index
14. silica # material name
```

```
15. 2.65 # dry density (g/cm3)
16. 0 # water content, % of dry mass
17. 1 # number of components
18. 1 100 # component index, % of dry mass
19. ### granulometry ###
20. 1 2.65 30.31 1 #grain component index, density, compacity
    (%), number of granulometric fractions
21. ### diameter in mm, volumetric fraction (%) of the total grains
    mass (sum must be equal to 100) ###
22. 0 0
23.
24. 1 # material index
25. surround_air # material name
26. 0.0013 # dry density (g/cm3)
27. 0 # water content, % of dry mass
28. 1 # number of components
29. 15 100 # component index, % of dry mass
30. ### granulometry ###
31. 0 0 0 0 #grain component index, density, compacity (%), num-
    ber of granulometric fractions
```

```
32. ### diameter in mm, volumetric fraction (%) of the total grains
    mass (sum must be equal to 100) ###
33.
34. 2 # material index
35. al2o3 # material name
36. 3.97 # dry density (g/cm3)
37. 0 # water content, % of dry mass
38. 1 # number of components
39. 2 100 # component index, % of dry mass
40. ### granulometry ###
41. 2 3.97 30.31 1 #grain component index, density, compacity
    (%), number of granulometric fractions
42. ### diameter in mm, volumetric fraction (%) of the total grains
    mass (sum must be equal to 100) ###
43. 0.4 100
44.
45. 5 5 5 # voxels number along X,Y and Z axes
46. 10 10 10 #voxels size along X,Y and Z axes (mm)
47.
48. ### MEDIUM COMPOSITION - cartography of materials with
49. their index
```

```
50.

51. 1 1 1 1 1

52. 1 1 1 1 1

53. 1 1 1 1 1

54. 1 1 1 1 1

55. 1 1 1 1 1

56.

57. 1 1 1 1 1

58. 1 1 0 1 1

59. 1 0 0 0 1

60. 1 1 0 1 1

61. 1 1 1 1 1

    ...

62. 1 1 1 1 1

63. 1 1 1 1 1

64. 1 1 1 1 1

65. 1 1 1 1 1

66. 1 1 1 1 1

67.

68. ### Define detector size ###
```

```
69.
70. 100 100 100 #box size inside the internal voxel, for X,Y,Z
    (in % of X,Y,Z voxel sizes)
71. 50 50 50 #offset of box location inside the internal voxel,
    for X,Y,Z in % of voxel dimensions
```

3.3 Output File

The simulation runs through the specified number of photons or particles. Results from the detector voxels are recorded in a result file, shown in Figure 3.2. The result file has seven columns: "depth (mm)" detailing the depth of the probe reading from the top, "Material_Num" listing the material index of the voxel centered at the reading, "Material_Name" giving the name of the material of the said voxel, "Density (g/cm^3)" giving the material density of said voxel, "Water_content (%)" giving the percent water makeup of said voxel, "Em-Mass (Gray)" listing the radioactive energy emitted by the voxel [1], and the "Dose_absorbed (Gray)" detailing the amount of radiation energy absorbed by the voxel.

[1] *Em_mass*is the energy per mass emitted by a voxel. If the voxel is not radioactive, then this value is 0.

3.3.1 Example Result File

depth(mm)	Material_Num	Material_Name	Density(g/cm3)	Water_content(%)	EmMass(Gray)	Dose_absorbed(Gray)
0.5	1	surround_air	0.0013	0	3.78927	4.72E-05
1.5	0	silica	2.65	0	0.00049438	8.44E-05
2.5	0	silica	2.65	0	0.000494284	8.06E-05
3.5	2	al2o3	3.97	0	0.000329975	6.47E-05
4.5	2	al2o3	3.97	0	0.000329938	6.55E-05
5.5	2	al2o3	3.97	0	0.000329955	6.63E-05
6.5	2	al2o3	3.97	0	0.00032999	6.68E-05
7.5	2	al2o3	3.97	0	0.000329981	6.70E-05
8.5	2	al2o3	3.97	0	0.000330082	6.68E-05
9.5	2	al2o3	3.97	0	0.000330001	6.63E-05
10.5	2	al2o3	3.97	0	0.00032995	6.55E-05
11.5	2	al2o3	3.97	0	0.000329957	6.47E-05
12.5	0	silica	2.65	0	0.000494375	8.06E-05
13.5	0	silica	2.65	0	0.000494335	8.44E-05
14.5	1	surround_air	0.0013	0	3.78927	4.62E-05

FIGURE 3.2: Example of a Result File

Chapter 4

Parameterization and basic simulations

In DosiVox the irradiation geometry is assembled from cubical volumes. Workarounds were needed to simulate the cylindrical containers and samples used in the OSL lab here at ECU, examples of which are shown in Figure 4.1 below. This chapter describes parameterization tests that were performed to optimize sample geometry.

FIGURE 4.1: An example of one of the cylindrical quartzite containers used in the OSL lab at ECU. To the bottom right is an example of a quartzite sample in the form of slices.

The cylindrical probe that provides dose information can measure a vertical profile along the entire length of the container, but is limited to one single voxel within the cross section.

A horizontal profile has to be put together from point-by-point simulations. The second part of the chapter describes a set of simulations to obtain a high-resolution horizontal cross section. The results illustrate edge effects upon transition from one material into another and allow to determine how many simulations are required to obtain sufficient resolution in a horizontal profile.

4.1 Optimizing matrix dimensions

Due to the reliance of DosiVox on matrices of cubic voxels, the implementation of a cylindrically (or spherically) shaped sample/container can only be approximated. This approximation was carried out by creating an array in Excel based on the would-be radii of the container and the sample desired to be simulated, and by using Boolean logic statements, as shown below. Here, *or* denotes the *outer radius* of the container and *ir* denotes the *inner radius*.

if $x^2 + y^2 > or^2$, *return air value,*

else if $x^2 + y^2 > ir^2$, *return container value,*

else return sample value

This approximation results in a pixelization of the matrices that could have an effect on the efficacy of the simulations. As such, a test was conducted to determine which matrix size would result in the most resolution while having the least effect on dose rate per particle. Four matrices were used: 15 voxels by 15 voxels, 25 voxels by 25 voxels, 35 voxels by 35 voxels, and 45 voxels by 45 voxels (shown in Figure 4.2).

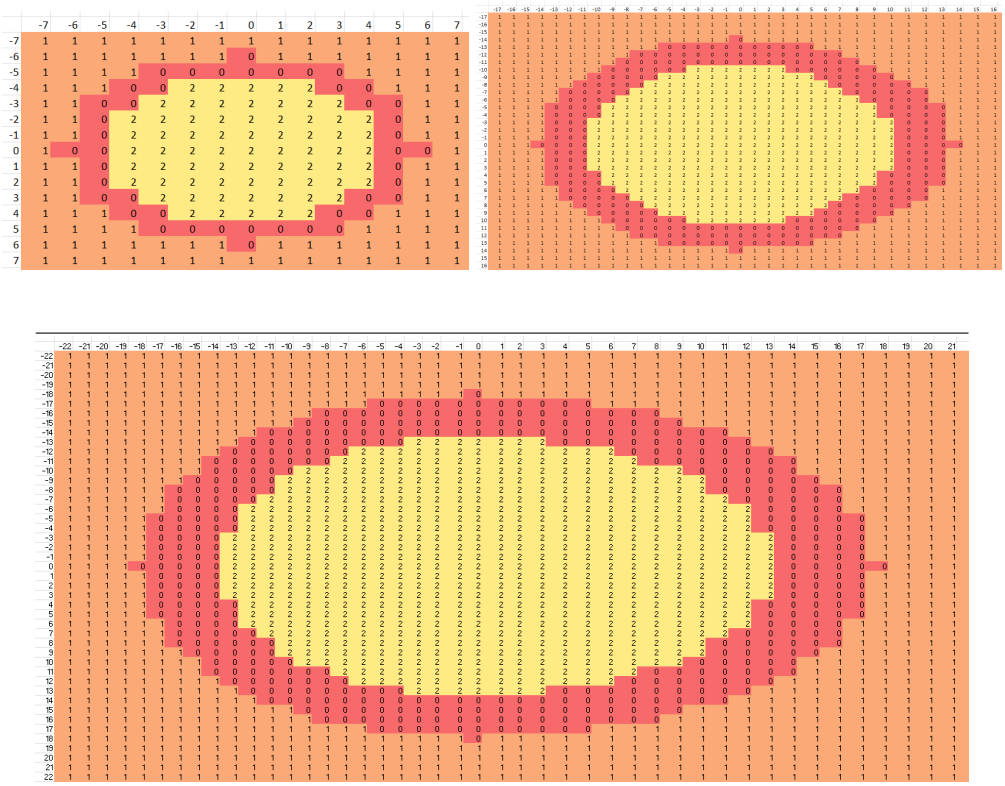

FIGURE 4.2: The matrices used in determining which matrix size produces the most statistically viable results. The numbers above and to the left of the matrix (in white) represents the distance from the center in *mm* in the x- and y-directions, respectively. The 15x15 square voxel matrix is shown to the top left, the 35x35 matrix to the top right, and the 45x45 matrix to the bottom.

Another set of matrices were simulated, all with a depth of 1 voxel. For each matrix, three simulations were run using different numbers of particles: one at 10,000 particles, another at 100,000 particles, and the other at 1,000,000 particles. The dose absorbed by the matrix from each of these three scenarios was plotted and used to make a linear regression, the R^2 and standard errors of which were recorded the Table 4.1 below. On the outset, one would expect the particle number and dose absorbed by the matrix to be proportional. This expectation holds true for all matrices, as the R^2 values of each linear fit are all very close to 1.

TABLE 4.1: R^2 Values by Dimension

Matrix Dimension	R^2 Values	Standard Error
15	0.999996897	6.87228×10^{-13}
17	0.999999939	9.42574×10^{-14}
19	0.999999997	2.17822×10^{-14}
21	0.999997799	2.17822×10^{-14}
23	0.999997946	5.65842×10^{-13}
25	0.999999995	2.80198×10^{-14}
35	0.999998935	4.02376×10^{-13}
45	0.999995517	8.36337×10^{-13}

This slope of each graph represents dose per particle (i.e. photon) per voxel. As voxel size decreases (and voxel number increases) the energy deposited in each voxel decreases. However, the mass of the voxel decreases as well. Dose is defined as energy per mass. To see if the dose would remain constant, or if it depends on voxel size, the resulting slope values were graphed against their associated matrix dimension. This graph, shown below in Figure 4.3, shows no clear relationship between dose per particle and matrix dimension. It was concluded that larger matrices do not impact the average dose, but provide higher resolution.

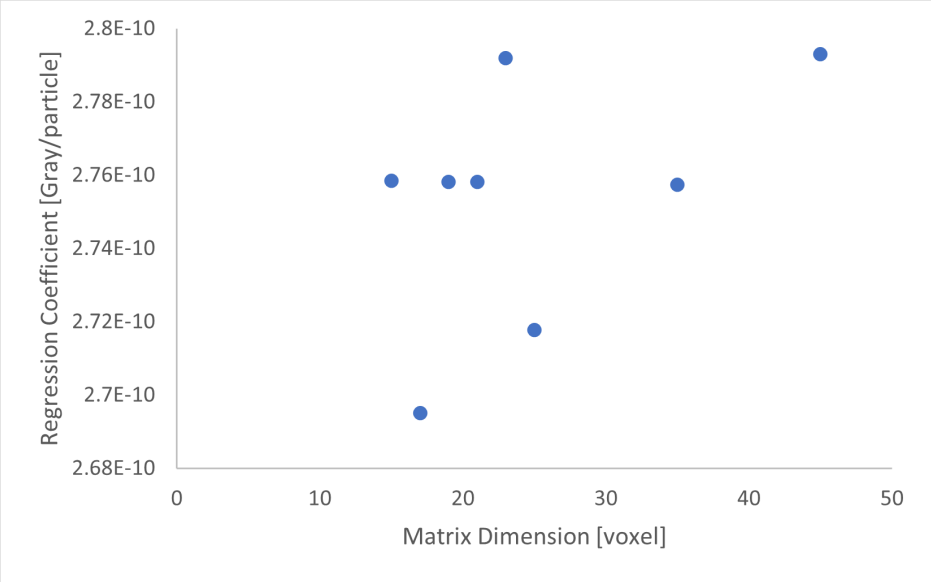

FIGURE 4.3: Regression Coefficients by Matrix Dimension

There are, however, more realistic limitations aside from resolution: the amount of time required for each simulation and the statistical fluctuations arising from the number of particles used. These factors operate in contrast with one another, since having more particles results in higher statistical significance but also takes more time to simulate.

As a result, another test was conducted. Simulations were performed with a volume of 51 by 51 voxel matrices stacked 51 voxels deep. These simulations ran for 10k particles, 100k particles, 500k particles, 750k particles, 1M particles, and 10M particles. As shown in Figure 4.4 below, there is a wide range in the times each number of particles takes, with the lowest running for 30 minutes and the highest running for 2 weeks.

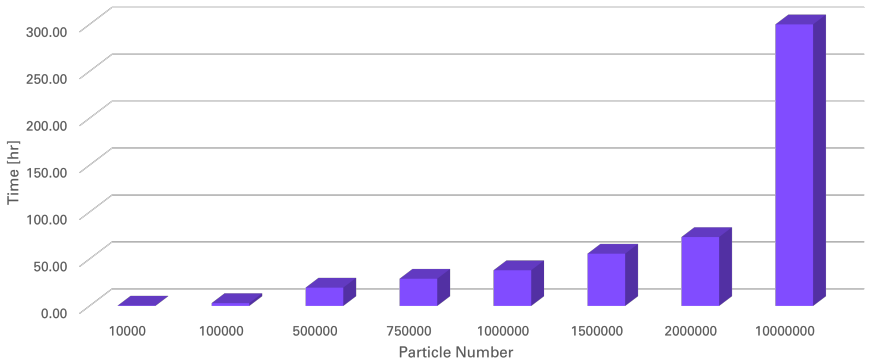

FIGURE 4.4: Time required for simulations by the number of particles simulated.

The resulting simulation outputs were analyzed by taking an average of all voxels inside the sample and calculating the standard error of the dose. These were graphed against the number of particles in the two plots given below as Figure 4.5.

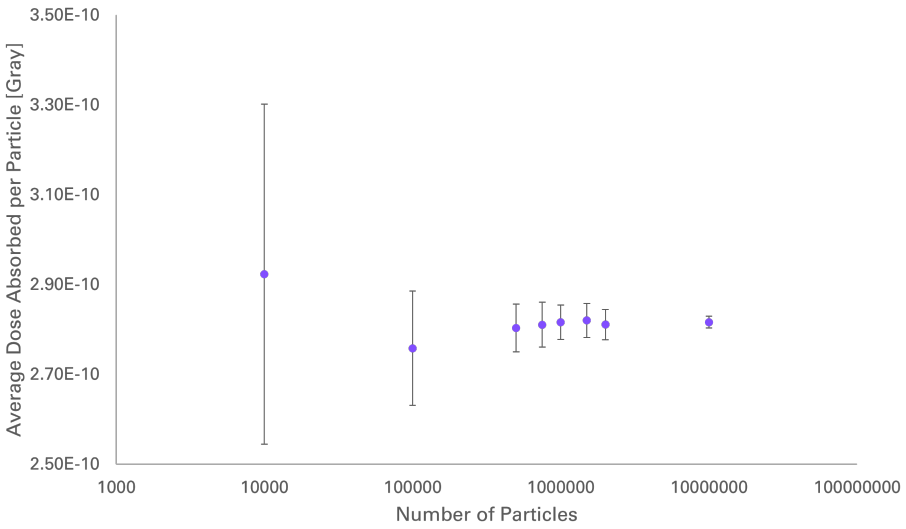

FIGURE 4.5: Statistical relevance for simulations determined by the amount of error for increasing number of particles.

As seen from the figure, statistical relevance begins to be maintained at 500k particles

and higher. This is reinforced by the tolerances, shown in Figure 4.5 above, also "level off" around the 500k particle mark. For practical reasons, it was determined that 500k particles was best for all upcoming simulations since it takes the least amount of time (about a day and a half) while still maintaining statistical relevance.

4.2 Edge Effects and horizontal cross sections

Secondary electron equilibrium is disturbed at the contact points between different materials.

To test the difference between the effects of similar and differing materials on the uniformity of dose received, three sets of simulations were run. Each set had 12 simulations, with each simulation having its probe at different distances from the center. In total, this effectively placed a probe reading every two voxels throughout the container and sample, with each voxel set to be 0.36 [mm] in length. Averaging each measurement produces a cross section of the cylinder, as shown in the orange section of Figure 4.6 below.

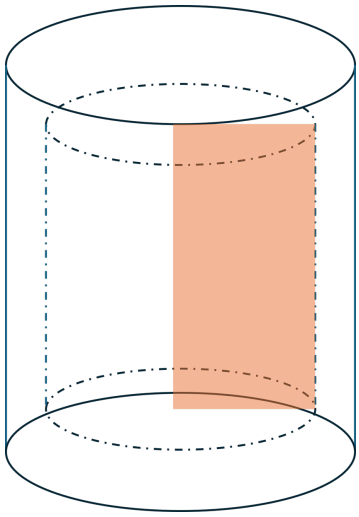

FIGURE 4.6: An illustration of a sample (dashed cylinder) inside a container (solid cylinder). The orange shaded area represents the radius and length that the probes cover.

The first set consisted of using Silica (SiO_2) for the container and Ceramic (Al_2O_3) for the sample. The edge separating the silica from the ceramic occurs at $5[mm]$ from the center. As can be seen in the resulting cross section shown in Figure 4.7 below, there is an edge effect between the silica and ceramic.

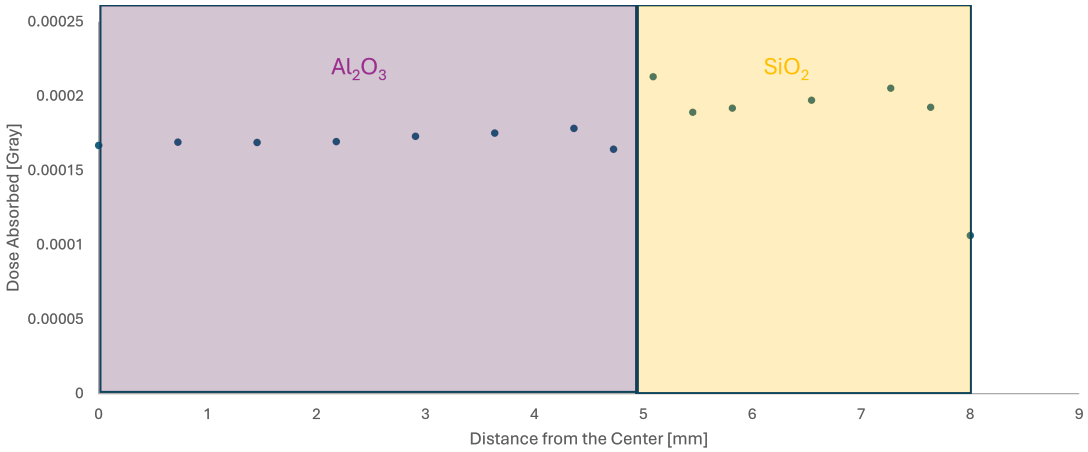

FIGURE 4.7: A graph detailing the dose absorption for different points along the radius of the sample and container. The ceramic sample can be seen on the left in purple, and the silica container on the right in gold.

The lower density silica shows an increase in absorbed dose at the container-sample interface, whereas the higher density ceramic shows a decrease in absorbed dose at the same edge. Similarly, swapping the materials (i.e. using silica for the sample and ceramic for the container) results in an even clearer edge effect, as seen in Figure 4.8 below. The higher density ceramic shows a decrease in absorbed dose at the edge, the lower density silica shows an increase in absorbed dose.

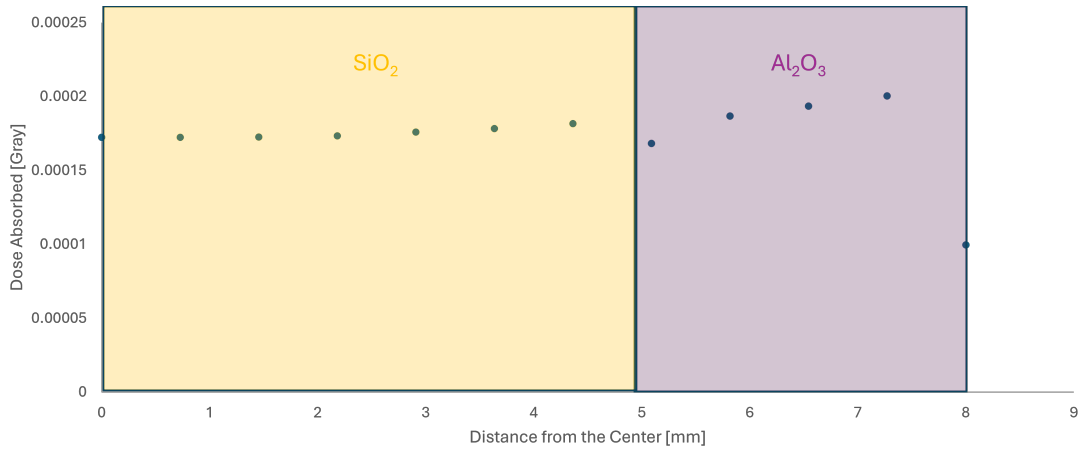

FIGURE 4.8: A graph detailing the dose absorption for different points along the radius of the sample and container. The silica sample can be seen on the left in gold, and the ceramic container on the right in purple.

For proof of concept, the third set of runs was conducted using ceramic for the container and the sample in order to simulate a situation in which the sample and container are the same material. As shown in Figure 4.9 below, the dose is visually uniform and shows no noticeable edge effects.

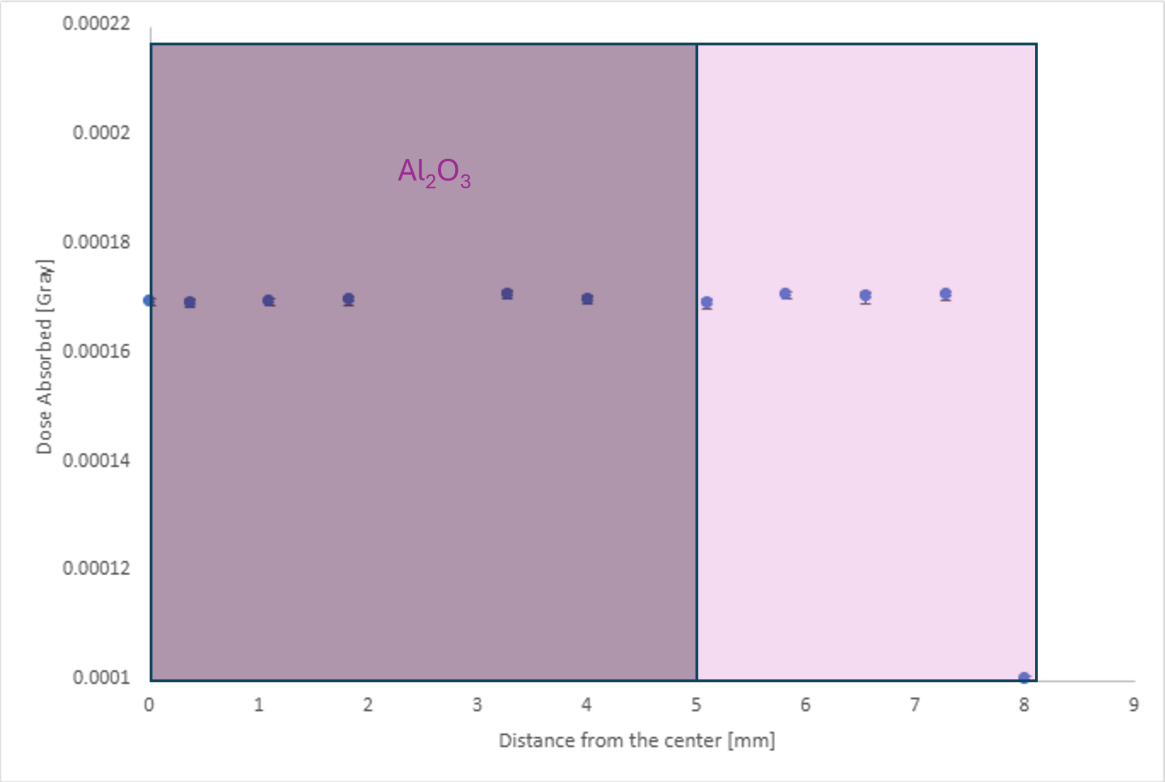

FIGURE 4.9: A graph detailing the dose absorption for different points along the radius of the sample and container. The ceramic sample can be seen on the left in dark purple, and the ceramic container on the right in light purple.

It should be noted here that the ptf used for the same materials case shown in Figure 4.9 is slightly different from the others in that the sample and container could **not** be specified as two separate materials. This, in effect, makes the simulation run the sample and container as one solid block of ceramic, which could affect how the software simulates what radiation effects occur at the sample-container interface.

4.2.1 Analysis

These edge effects arise from the movement and trapping of the free electrons discussed in Chapter 2. The higher the density of a material is, the more matter there is that free electrons have to navigate which hinders free electron movement.

As the materials are irradiated, a higher density material (e.g. ceramic) will lose free electrons to the lower density material (e.g silica) near the interface between them, since electrons will be less hindered as they move from the higher density material to the lower density material but would be more hindered upon a return trip.

As such, more free electrons find themselves becoming trapped in the lower density material than in the higher density material near the interface. This can be seen in Figure 4.7, with ceramic showing a decrease in absorbed dose (i.e. trapped free electrons resultant from irradiation) at the sample-container interface and ceramic showing an increase in absorbed dose on the other side.

This is also seen in the furthest point in all three graphs (Figures 4.8, 4.7, and 4.9) where the container has an interface with air. Air has an extremely low density, far lower than either ceramic or silica, which causes a drastic decrease in absorbed dose at the container's outer edge.

These edge effects have a direct effect on the uniformity of dose absorbed with a contained material. It is the goal of this study to determine which materials result in the least effects on dose uniformity within common sample materials.

Chapter 5

Data Analysis

The simulation results provided vertical profiles for distinct voxels on a horizontal cross section of the container. When OSL measurements are performed, the average dose of the entire container is obtained. Thus the simulation results have to be combined in such a way to provide average dose over the entire container and a standard deviation to quantify uniformity. This chapter describes the mathematical procedure that was used to calculate dose and standard error.

5.1 Apparatus for Data Analysis

The average dose absorbed by the total sample volume had to be calculated in a way that accounted for the cylindrical shape of the samples, taking into account that only data for discrete points were available. Average doses were first calculated for one single layer, and in a second step for the entire stack (i.e. the entire sample). It was determined that a weighted average must be calculated for each radial probe location. Each probe represents the dose absorbed by any arbitrary point on that specific radius. Furthermore, the probe value will not only represent an infinitely narrow circle, but it will represent a ring, the width of which

depends on the distance to the neighboring probes. The average dose absorbed at a certain probe radial point should therefore be weighted as a ring at that point.

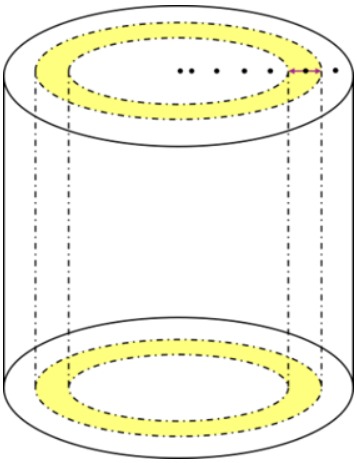

FIGURE 5.1: A graphic of a cylindrical sample showing the radial points used for each probe location and the weighted ring covered by one of those points

This gives a weighting of $2\pi r\,dr$, where r is the radius (i.e. distance of the probe from the center) and dr is the thickness of the ring that the probe accounts for (indicated by the red arrows in Figure 5.1). Since everything is in terms of voxels, r must be the average radial distance that each voxel accounts for. A set of seven simulations was conducted for each scenario with cylindrical probes at a distance of $4.00[mm]$, $3.27[mm]$, $2.55[mm]$, $1.18[mm]$, $1.09[mm]$, $0.36[mm]$, and $0.00[mm]$. Thus the average radial distance can be calculated using the following equation

$$r = \frac{r_1 + r_2}{2}$$

where r_1 and r_2 are the maximum and minimum radii that the voxel covers. As such, dr may be calculated by $dr = r_2 - r_1$.

To average over the entire disk (indicated by the yellow areas shown in Figure 5.1), all rings need be summed and this sum divided by the area of the disk.

$$D_r = \frac{1}{\pi R^2} \sum_{i=1}^{7} d_i 2\pi r_i \, dr_i$$

Here, D_r is the average dose absorbed in the disk and R is the largest average radius. For use in the sum, r_i represent the radial distances of the various probe positions and dr_i the thickness of the associated rings. As well, d_i represent the dose measured in the respective voxel.

A final average must then be taken for each disk to account for the total Dose absorbed by the cylinder. This average can be taken using

$$D = \frac{\sum_r^n D_r}{n}$$

where n is the number of layers of disks and D_r is the average dose of the disk.

The standard deviation proved much trickier to elucidate. The nature of the standard deviation is to quantify how much each point deviates from the mean. Under normal circumstances, this may be calculated as

$$\sigma = \sqrt{\frac{\sum_i (x_i - \bar{x})^2}{N}}$$

with x_i being the point in question, $\bar{x}$ the average of all points, and N the number of points [9]. In our case, however, the weighting of each ring must be taken into account, as well as the area of each disk. The standard deviation now becomes

$$\sigma = \sqrt{\frac{\sum_{i,k} 2\pi r_k (d_i - D)^2 \, dr_k}{\pi R^2 N}}$$

where r_k is the average radius between two adjacent radii, dr_k is the distance between those two radii, d_i is the dose measured in the voxel at the max of those two radii, and D is the

average dose of the whole sample. From this, the standard error (err) and relative standard deviation (RSD) may be calculated as normal via the equations below [10].

$$err = \frac{\sigma}{\sqrt{N}}$$

$$RSD = \frac{\sigma}{D} \times 100\%$$

Chapter 6

Results

In previous chapters, the geometry for simulating the irradiation of different sample-container setups was parameterized. The data analysis procedure was explained. In this chapter, we will discuss the results of these simulations and what these results indicate with regard to dose uniformity.

6.1 The Uniformity of Different Setups

Simulations were conducted for two sample materials: ceramic (Al_2O_3) and silica (SiO_2). For each, there was a set of simulations done with containers made of aluminum, teflon, glass [1], ceramic, and silica.

These sets consisted of seven separate runs, each run with a different probe location along the radius of the sample (from center to edge). An average dose was found along the length of each probe, then a weighted average was taken of all seven probes according to the analysis discussed in Chapter 5.

[1]The glass used here is borosilicate glass composed of the following: 80% SiO_2, 13% B_2O_3, 4% Na_2O, and 3% Al_2O_3, al with a dry density of 2.2 $[g/cm^3]$ [11].

For each weighted average, a standard deviation and relative standard deviation were calculated. These averages and calculations were tabled for each sample material in Tables 6.1 and 6.2 below.

TABLE 6.1: Ceramic Sample Results

Material	Dose absorbed [Gy]	RSD
Aluminum	2.23×10^{-5}	2.18%
Silica	2.33×10^{-5}	2.48%
Ceramic	8.38×10^{-5}	2.65%
Glass	2.38×10^{-5}	3.38%
Teflon	5.07×10^{-5}	4.94%

TABLE 6.2: Silica Sample Results

Material	Dose absorbed [Gy]	RSD
Glass	2.80×10^{-5}	2.87%
Silica	8.78×10^{-5}	3.09%
Ceramic	2.69×10^{-5}	3.65%
Teflon	5.92×10^{-5}	4.39%
Aluminum	2.56×10^{-5}	5.91%

In both cases, relative standard deviation (as derived from the weighted standard deviation discussed in Chapter 5) is used as a quantified measure of uniformity, with high uniformity being defined as having the lowest relative standard deviation.

For Ceramic (Al_2O_3) samples, it can be seen that the container material with the lowest RSD is aluminum, followed by silica and ceramic. Glass has a higher RSD than any of the

previous materials, making it the material with the second largest non-uniformity of absorbed dose.

For Silica (SiO_2) samples, the container material with the lowest RSD is glass, followed by silica and ceramic. Aluminum has the highest RSD in this case, making it the material with the most non-uniform absorbed dose.

For both sample materials, Teflon has one of the highest amounts of non-uniformity of absorbed dose by a drastic margin.

It may also be noticed that for both samples, having a container of Teflon resulted in similar measurements of absorbed dose. This dose is almost twice as large as the dose for the other materials. As well, both cases of the sample and container being the same resulted in similar dose measurements, however, both being ~ 3 times larger than the dose measured in the lowest RSD material.This observation cannot be easily explained and more simulations are necessary to verify and investigate this observation.

6.2 Conclusion

For both sample materials, it can be argued that the worst option of container materials is Teflon. The amount of variation of absorbed dose within the either types of sample is extremely high and would be most likely to cause inaccuracies within calibration calculations.

In any case, the material that would result in the absolute highest amount of uniformity of absorbed dose throughout the sample is *not* the same material. The best for ceramic samples is actually *aluminum metal* and the best for silica is *borosilicate glass*, rather than ceramic and silica respectively.

Given that the simulations where the sample and container are the same were conducted using one solid block of material, there is a likely possibility that the variance found in

uniformity of sample dose is caused by the scatter inherent to the simulation software. This would indicate that the uniformity of sample dose that is found to have less variance (like borosilicate glass for silica sample) than the same material setups is likely the same since it represents the inherent scatter.

Ergo, it would be as beneficial for uniformity to use a glass container for a silica sample as it is to use a silica container. Similarly, it would be as beneficial to use an aluminum container for a ceramic sample as it is to use a ceramic container. As both aluminum and glass are readily available and cheap, they can be used to hold loose grains and slices alike of their respective sample material counterparts without any loss in uniformity.

6.2.1 Future Directions

As is always the case with simulation-based work, a study can always benefit from more simulations being conducted on bigger scales. Simulating more sample-container setups at higher numbers of particles would reduce any variance caused by the simulations themselves, which would further accentuate and clarify the levels of uniformity.

In the case of this particular study, there would have been a tremendous benefit in conducting more simulations of the same setups multiple times as it would have provided a clearer determination of the scatter inherent to the simulation software. Thus, a future study could repeat these simulations a multitude of times in order to calculate an error range that would be used to quantify the inherent scatter for use in direct comparison. This would help in proving the reliability of the results of this study.

Another issue in this study that was not able to be addressed in time is the fact that the cutoff length (shown in Line # of Chapter 3) may have been too short for the software to properly simulate. A future study could benefit from utilizing a cutoff of $0.1[mm]$ instead of $0.36[mm]$ which was used here.

The next big step in such a study as this one is to corroborate the simulated doses found for each setup with real measurements. Such measurements would be useful in determining the extent of applicability of the results of this study, as well as giving the study an added layer of legitimacy.

Bibliography

[1] M. Autzen, C. Andersen, M. Bailey, and A. Murray, "Calibration quartz: an update on dose calculations for luminescence dating", Radiation Measurements **157**, 106828 (2022).

[2] N. W. Ashcroft and N. D. Mermin, *Solid state physics*, 1st ed. (Harcourt College Publishers, 1976).

[3] "Chapter 6 - interaction of gamma quanta with matter", in *Radiation*, edited by I. Obodovskiy (Elsevier, 2019), pp. 137–150.

[4] F. H. Attix, *Introduction to radiological physics and radiation dosimetry* (Wiley-VCH, 1986).

[5] E. J. Rhodes, "Optically stimulated luminescence dating of sediments over the past 200,000 years", Annual Review of Earth and Planetary Sciences **39**, 461–488 (2011).

[6] L. Martin, S. Incerti, and N. Mercier, "Dosivox: implementing geant 4-based software for dosimetry simulations relevant to luminescence and esr dating techniques", Ancient TL **33** (2015).

[7] G. I. Collaboration, "Introduction to geant4", Geant4 Documentation **11.2** (2023).

[8] L. Martin and N. Mercier, *Dosivox manual* (Universite Bordeaux Montaigne Maison de l'Archeologie, 2019).

[9] B. Illowsky and S. Dean, *Introductory statistics* (Rice University OpenStax, 2018).

[10] M. L. Boas, *Mathematical methods in the physical sciences*, 3rd ed. (Wiley, reprint 2015).

[11] M. Hasanuzzaman, A. Rafferty, M. Sajjia, and A.-G. Olabi, "Properties of glass materials", in *Reference module in materials science and materials engineering* (Elsevier, 2016).